

THIN-FILM SOLID-STATE RECHARGEABLE LITHIUM BATTERY

J. F. Ribeiro¹, M. F. Silva¹, L. M. Goncalves¹, J.P. Carmo¹, J. H. Correia¹,
M. M. Silva², F. Cerqueira³, P. Alpuim³, J.-E. Bourée⁴

¹University of Minho, Algoritmi Centre, Guimarães, Portugal

²University of Minho, Chemistry Centre, Braga, Portugal

³University of Minho, Physics Centre, Braga, Portugal

⁴Lab. de Physique des Interfaces et des Couches Minces, CNRS UMR 7647, E. Polytechnique, France

Abstract — This paper describes the optimization and the materials technology required for fabricating thin-film solid-state rechargeable lithium batteries. The following materials were selected, deposited and optimized: a glassy lithium-phosphorus oxynitride electrolyte (LiPON) between a lithium (Li) anode and crystalline lithium-cobalt dioxide cathode (LiCoO₂), deposited by RF-sputtering. Ti/Pt layers, deposited by evaporation (using the e-beam technique) were used in contacts and a silicon nitride thin film (Si₃N₄), deposited by Hot-wire CVD protects the battery. This technology allows batteries with a potential of 4.5 V, typical capacities of 50 μA.cm⁻² and charge discharge rates up to 4C.

Keywords : Solid-state, thin-film battery, materials technology, lithium, energy-harvesting, microsystems

I – Introduction

It's undeniable the fact that batteries are systems with the highest number of applications known up to know. Since the invention of the first pile by Volta on 1800, batteries are used in applications that range from vehicles to the most modern cell phones, toys/gadgets and biomedical devices. Despite the developments made by the microelectronic industry, the battery technology didn't accompany these breakthroughs [1]. The increased demand of stand-alone microsystems in critical energy applications, such as radio-frequency identification tags, integrated circuit smart cards [2], data acquiring systems on extreme industrial harsh environments, oil drilled sinks and wireless sensor networks, led to the investigation and development of solid-state rechargeable batteries [3]. In energy harvesting systems, thin-film batteries of solid-state materials are suitable power sources to fill the time gaps, when the external power source is not available, thus assuring that microsystems are still powered and active. This is of special concern when the target applications are in the biomedical field or for long cycle operations without requiring human activity [4, 5].

Two forms of film batteries have been developed so far: the polymer based lithium batteries and the film lithium batteries. The polymer batteries (that are already common in the market) have high capacity and stability but low charge/discharge rates, mainly due to temperature limits. Solid-state film batteries show faster charge rates and very high cycle life, compared with classical liquid electrolyte batteries, withstanding several thousands of cycles with no pronounced fading. The integration of batteries with solid-state circuits requires the use of

solid-state anode, cathode and electrolyte. These batteries are intrinsically safe since all materials are solid and no leaking or explosion could occur. Moreover, this technology allows the fabrication of batteries that are not damaged during the soldering process of microchips. Film battery chemistry is being developed at ORNL (Oak Ridge National Laboratories) [4] with a solid electrolyte between the anode and cathode. These batteries have a potential of 4.5 V, typical capacities below 100 μAcm⁻² and charge times of 2C to 5C. As illustrated in Figure 1, the film batteries present the highest volumetric energy density (800 Whl⁻¹) and gravimetric energy density (350 Whg⁻¹) and charge-discharge rates up to 5C (only exceeded by super-capacitors) [6, 7]. However, due to the process of deposition of thin-films, the thickness is limited to few micrometers, resulting in a small capacity. The market of film batteries is in the trial stage and it's predictable to reach 10 billion units by 2012.

This paper presents the fabrication process and characterization details of all materials used in a thin-film lithium rechargeable battery for integration with stand-alone microsystems.

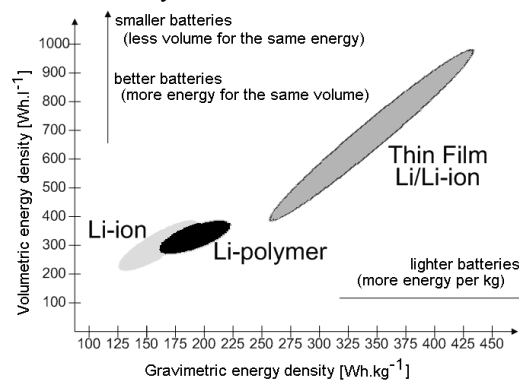


Fig 1: Size and capacity with different battery technologies.

II – Materials Selection

The integration of batteries with solid-state circuits requires the use of solid-state anode, cathode and electrolyte. The Figure 2 shows an artwork of a film battery fabricated by successive layers deposition on top of a silicon compatible substrate (among the glass, the [100] undoped double-side polished silicon wafer was used for thin-films depositions). The first layer are the battery contacts, and platinum was chosen for allowing a good distribution of electrons trough the cathode surface without reacting with it. The cathode is a lithium cobalt dioxide (LiCoO₂) thin-film; the electrolyte is a glassy lithium-phosphorus oxynitride electrolyte (LiPON) thin-film and anode is a lithium (Li) thin-film. The

protection layer is a silicon nitride (Si_3N_4) thin-film [8]. This protective layer avoids the reaction of lithium with air.

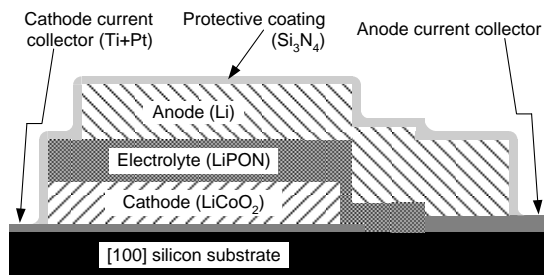


Fig 2: Artwork of a thin-film battery.

The operation of lithium batteries is based on reversible insertion and removal of lithium ions to and from their positive and negative electrodes [9]. Metals that are compounds of lithium (Li) and presents a layered structure, especially the ones containing 3D transition metals such as nickel (Ni), manganese (Mn), vanadium (V) and cobalt (Co). The lithium oxides containing these materials are excellent candidates as active compounds for use as high capacity cathode materials due to their high energy density, a long life cycle, a very good safety, constant discharging properties and a wide range of operation temperatures [10], without compromising the structural stability [11]. Compared with other materials such as the LiMn_2O_4 and LiNiO_2 , the LiCoO_2 is easy to fabricate and has a relatively high charge storage capacity (140 mAhg^{-1}).

Thin-film solid electrolytes are required to have high ionic conductivity, a negligible electronic conductivity and be stable in contact with the anode and cathode electrodes [7] that will allow for a high current capacity and low self-discharge current, respectively. As suggested by Hamon et al [12], the LiPON films with an amorphous structure are the most suitable candidates for obtaining films with high ionic conductivity when compared with crystalline structures. LiPON films present an exceptional electrochemical stability, an electronic resistivity greater than $10^{12} \text{ } \Omega\text{m}$ and ionic conductivity in of 10^{-6} Scm^{-1} range. Films of LiPON can be obtained by RF sputtering of a lithium phosphate (Li_3PO_4) target in an argon (Ar)/nitrogen (N_2) plasma. Behind electronic properties, LiPON have low stress (typically, less than 100 MPa) and a good stability in air atmosphere [13].

The transition metal oxides were used as anode materials in previous works [14, 15], as it is the case of the tin dioxide (SnO_2). However, this compound presents a serious problem related with an irreversible reaction during the first battery charge, resulting in small clusters of tin metal (Sn) with lithium oxide (Li_2O). An anode material with higher degree of reversibility results in a battery with higher specific capacity. For this reason, the lithium (Li) metal was selected for the anode material, but also because it exhibits the highest capacity and discharge rate despite the fast oxidation in contact with the air. A way to overcome the last drawback is covering the battery with a protective layer of silicon nitride (Si_3N_4). Multilayers of SiN_x thin films are used to achieve higher protection against moisture and avoid reaction with air. Each layer has a low-frequency Ar-plasma treatment for surface compaction.

II - Fabrication Details

On top a silicon wafer where a thin layer of dioxide was grown by thermal oxidation, the current collector (contact) of platinum (100 nm) was deposited by e-beam. A titanium (Ti) layer with a thickness of 30 nm was previously deposited to improve the adhesion of the platinum to the substrate.

The $1 \text{ } \mu\text{m}$ thick LiCoO_2 cathode was deposited by RF magnetron sputtering technique using a RF power source 13.56 MHz at 150 W, a pressure of 0.2 Pa in a 30 sccm flow of argon (Ar) and 10 sccm flow of oxygen (O_2). A deposition rate from $3.5 \text{ } \text{Ås}^{-1}$ to $4.5 \text{ } \text{Ås}^{-1}$ was obtained. This process is still the most effective way to provide the required crystalline structure of LiCoO_2 films. The best annealing temperature was found experimentally using a different temperatures (from $500 \text{ } ^\circ\text{C}$ to $800 \text{ } ^\circ\text{C}$), during 30 minute, in vacuum.

The electrolyte (LiPON) was deposited by RF magnetron sputtering technique with $1 \text{ } \mu\text{m}$ thickness. A Li_3PO_4 target was used in a 20 sccm reactive Ar/ N_2 plasma. The depositions were done with controlled: the pressure inside the deposition chamber (from 0.03 Pa to 1 Pa) and controlled power in the RF source (13.56 MHz) of the sputtering system (150W to 200W), with a deposition rate from $0.4 \text{ } \text{Ås}^{-1}$ to $2.5 \text{ } \text{Ås}^{-1}$.

The lithium anode was deposited by thermal evaporation, in a large molybdenum boat (3 cm^3). A base pressure of 10^{-6} mbar and a deposition rate of $30 \text{ } \text{Ås}^{-1}$ were measured.

A thin layer of Si_3N_4 is deposited just after lithium (without open the chamber). This layer (100 nm) is deposited by RF magnetron sputtering technique at 300 W, a pressure of 0.2 Pa in a 20 sccm flow of N_2 . This layer offers the necessary air protection to transfer the battery to the Hot-wire chemical vapor deposition (HWCVD) chamber, where the silicon nitride capping multilayer is deposited. These were obtained by using a sequence of HWCVD deposition of the SiN_x followed by a low-frequency (100 kHz) Ar-plasma treatment for surface compaction. The final thickness of the structure was 120 nm, composed of $4 \times 30 \text{ nm}$. The HWCVD deposition of SiN_x was performed at 25 mTorr from silane and ammonia gaseous mixtures using two hydrogen dilutions, namely 88% and 90%. The Ta current filament was 16 A, corresponding to a filament temperature of $2000 \text{ } ^\circ\text{C}$. The Ar treatment was performed at 230 mTorr using a pulsed source for a short time. The sequence of SiN_x deposition and Ar treatment was performed without breaking the vacuum, by moving the sample between two twin chambers connected by a gate valve. For each hydrogen dilution, two samples were deposited under a different NH_3 to SiH_4 flow rate ratio, R, namely $R = 2$ and $R = 3$, so fabrication receipt could be tuned.

IV –Results and Discussion

A. LiCoO_2 cathode

The Figure 3 shows the X-ray diffraction (XRD) spectrum of the LiCoO_2 films for three annealing temperatures ($600 \text{ } ^\circ\text{C}$, $650 \text{ } ^\circ\text{C}$ and $700 \text{ } ^\circ\text{C}$). The joint analysis between the diffractograms of the Figure 3 and the peak positions of planes [003], [101], [104], [018] and

[110] confirms the predominance of crystalline LiCoO_2 in the composition of the selected samples (diffraction patterns 016-0427 [16] were used in crystallographic analysis).

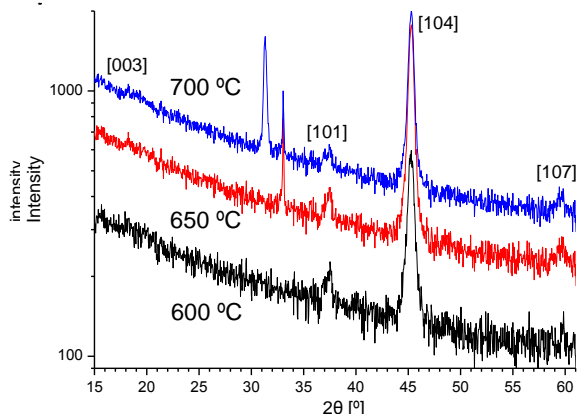


Fig 3: XRD spectrogram of three LiCoO_2 films annealed at different temperatures (600 °C, 650 °C and 700 °C).

In the Figure 3 it is also possible to observe the evolution of LiCoO_2 peaks in XRD pattern with the increase in the annealing temperature. The annealing temperature increase resulted in a polycrystalline structure with strong orientation in the [104], [018] and [110] planes and fewer at [003] and [101] planes as it was presented before [17]. This structure improves the ion diffusing, thus increasing ionic conductivity and ion insertion and extraction. However, a phase transition occurs at 650 °C, as depicted in Figure 4. The in-plane resistivity was measured using the Van der Pauw technique, for LiCoO_2 samples annealed at different temperatures (see the Figure 4).

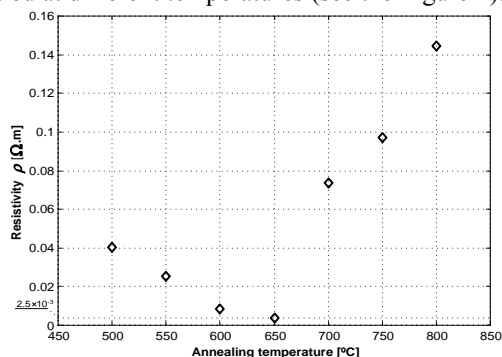


Fig 4: Resistivity of LiCoO_2 samples, as function of annealing temperature.

A decrease of resistivity was found with an increase of annealing temperature. The minimum resistivity value of $2.5 \times 10^{-3} \Omega\text{m}$ was measured (at room temperature) in sample annealed at 650 °C. However, for annealing temperature above 650 °C, the resistivity rapidly increases with annealing temperature. This behavior was also reported before [17].

B. LiPON electrolyte

The ionic conductivity of LiPON was measured on the best samples with the procedure described [12]. A sinusoidal voltage with amplitude of 25 mV (peak to peak) was used to measure the impedance of the sample at several values of frequency (from 0.5 Hz to 65 kHz). The inset in Figure 5 shows the LiPON thin-film with top and bottom contacts of platinum (Pt) for measuring the ionic

conductivity. Both real (Z') and imaginary (Z'') parts of the impedance were respectively projected in x-axis and y-axis, in order to obtain a two dimensional Nyquist plot.

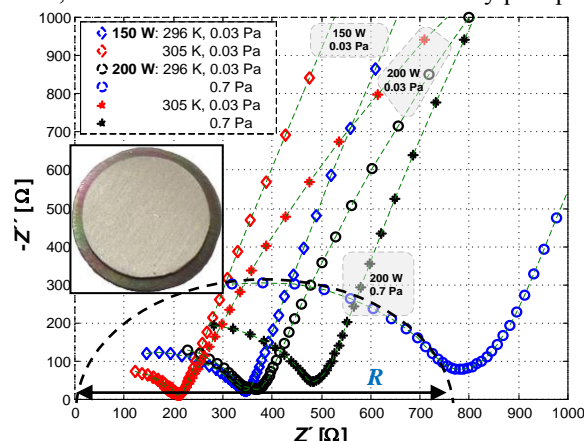


Fig 5: Typical Nyquist plots of LiPON samples.

Nyquist plots (measured at temperatures of 296 K and 305 K) are presented in Figure 5, for samples deposited at N_2 pressures of 0.03 Pa and 0.7 Pa, with RF sputtering power of 150 W and 200 W. The diameter of each semi-circle indicates the resistance of the electrolyte (R), whose values were obtained with the help of Autolab software.

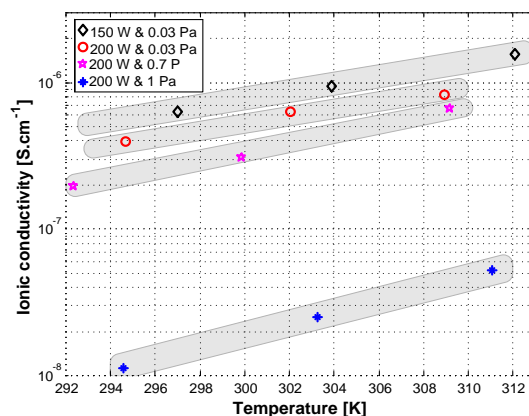


Figure 6: Ionic conductivity of LiPON thin-films.

Considering the area (A) and the thickness (d) of the electrolyte, the ionic conductivity, σ [$\text{S}\cdot\text{cm}^{-1}$], of LiPON is given by $\sigma = d/(A \cdot R)$ where R [Ω] is the resistance from Nyquist diagram. The best ionic conductivity archived was between $10^{-7} \text{ S}\cdot\text{cm}^{-1}$ and $10^{-6} \text{ S}\cdot\text{cm}^{-1}$. The Figure 6 shows the ionic conductivity of LiPON films deposited at N_2 pressures from 0.03 Pa to 1 Pa and with RF power of magnetron sputtering from 150 W to 200 W, measured in temperature range of 292 K to 312 K. The highest ionic conductivity of LiPON ($10^{-6} \text{ S}\cdot\text{cm}^{-1}$ at 304 K) was measured in the sample deposited at N_2 pressure of 0.03 Pa and a RF power of 150W. It was observed the decreases of ionic conductivity with increase of power or pressure.

C. Li anode

The Li resistivity was measured during the deposition using a four point setup and values around $10 \mu\Omega\text{m}$ were measured for 3 μm thick film. After the deposition, the resistivity of Li was measured at room temperature and atmospheric pressure without any protective layer in order

to evaluate the oxidation of Li. These results show that a protective layer is essential to keep the battery functional.

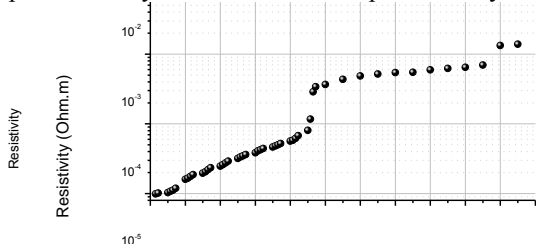


Fig 7: Evolution of lithium resistivity in contact with air.

D. Silicon nitride capping layer

Multilayers of SiNx thin-films, having refractive index of 2 (at 650 nm), were obtained. The final thickness of the structure was 120 nm, composed of 4×30 nm. All the samples are highly transparent in the visible/NIR range reaching more than 85% of transmission at 650 nm. The spectral refractive index was obtained from the transmission spectra in the visible and near infrared range (from 250 to 2500 nm) [18]. The multilayers will be electrically characterized by measuring the disruption field and the transport mechanism in the dielectric, under low and high applied electric field, in metal-insulator-metal (MIM) patterned structures defined lithographically. The quality of the multilayer as a device encapsulation barrier will be tested by measuring the water vapor transmission rate using the calcium test. The best samples will then be grown on top of the battery and the lifetime of the battery will be compared with that of batteries without encapsulation.

E. Battery

A battery, including all described materials, was fabricated using shadow masks to pattern different regions. Figure 8 shows a SEM image of the battery.

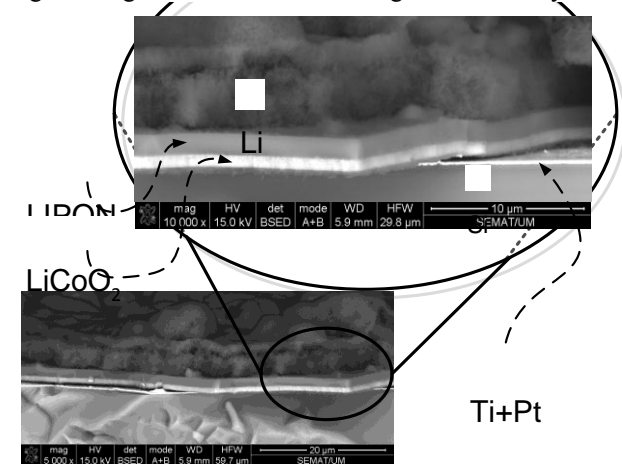


Fig 8: Cross-sectional SEM image of the thin-film battery.

IV - Conclusions

This paper presented the materials technology of rechargeable solid-state film lithium batteries for integration in stand-alone harvesting microsystems.

The RF magnetron sputtering, the e-beam evaporation and Hot-wire CVD were the techniques used for depositing the successive layers of the battery. The elements of the film battery are a LiCoO₂ cathode, a LiPON amorphous electrolyte and a Li anode. The

contacts are made of platinum and battery is protected with a Si₃N₄ layer. The best LiCoO₂ films, annealed at 650°C showed a resistivity of 0.25 Ωm. The best LiPON films have an ionic conductivity of 10⁻⁶ Scm⁻¹ (at 304 K), obtained from a deposition at 20 sccm of N₂ with a pressure of 0.03 Pa and with an applied power of 150 W. The Li anode was deposited by thermal evaporation and presents a low resistivity (10 μΩm). However, a rapid oxidation of Li occurs in contact with atmosphere, so a protective layer must be deposited at the same run. These materials have as good properties as standard large sized batteries and are suitable for the fabrication of solid-state lithium film batteries.

Acknowledgements

This work was financially supported by FEDER/COMPETE and FCT funds with the project PTDC/EEA-ELC/114713/2009.

References

- [1] M. Armand, and J. M. Tarascon, "Building better batteries", Nature, Vol. 451, pp. 652 657, 7 February 2008.
- [2] H. Nishide, and K. Oyaizu, "Toward flexible batteries", Science, Vol. 319, pp. 737 738, 8 February 2008.
- [3] J. P. Carmo, L. M. Gonçalves, and J. H. Correia, "Thermoelectric microconverter for energy harvesting systems", IEEE Transactions on Industrial Electronics, Vol. 57, No. 3, pp. 861 867, March 2010.
- [4] N. J. Dudney, and B. J. Neudecker, "Solid state thin films lithium battery systems", Solid State & Materials Science, Vol. 4, pp. 479 482, 1999.
- [5] B. Kang, and G. Ceder, "Battery materials for ultrafast charging and discharging", Nature, Vol. 458, p. 190, 2009.
- [6] N. J. Dudney, "Solid-state thin-film rechargeable batteries", Materials Science and Engineering – B, Vol. 116, pp. 245 249, 2005.
- [7] A. Patil, *et al.*, "Issue and challenges facing rechargeable thin film lithium batteries", Materials research bulletin, Vol. 43, pp. 1913 1942, 2008.
- [8] P. Alpuim, *et al.*, "Deposition of silicon nitride thin films by hot-wire CVD at 100 °C and 250 °C", Thin Solid Films, Vol. 517, pp. 3503 3506, 2009.
- [9] B. L. Ellis, K. T. Lee, and L. F. Nazar, "Positive electrode materials for Li-ion and Li-batteries", Chemistry of Materials, Vol. 22, No. 3, pp. 691 714, 2010.
- [10] L. Predoana, *et al.*, "Electrochemical properties of the LiCoO₂ powder obtained by sol gel method", J. of the European Ceramic Society, Vol. 27, pp. 1137 1142, 2007.
- [11] L. Predoana, *et al.*, "Advanced Techniques for LiCoO₂ Preparation and Testing", in Proc. International Workshop Advanced Techniques for Energy Sources Investigation and Testing, Sofia, Bulgaria, September 2004.
- [12] Y. Hamon, *et al.*, "Influence of sputtering conditions on ionic conductivity of LiPON thin films", Solid State Ionics, Vol. 177, pp. 257 261, 2006.
- [13] S. Oukassi, *et al.*, "Above IC micro power generators for RF MEMS", in Proc. Symposium on Design Test Integration and Packaging of MEMS/MOEMS (DTIP of MEMS & MOEMS), Stresa, Italy, pp. 1 4, April 2006.
- [14] J. P. Carmo, *et al.*, "Integrated thin-film rechargeable battery in a thermoelectric scavenging microsystem", in Proc. Powereng 2009, Lisbon, Portugal, pp. 359 363, 2009.
- [15] J. P. Carmo, *et al.*, "Sputtered SnO₂ for application in thin-film solid state microbatteries", in Proc. Materiais 2009, Lisbon, Portugal, April 2009.
- [16] Powder Diffraction File, Joint Committee on Powder Diffraction Standards, ASTM, Philadelphia, PA, 1967.
- [17] J. B. Bates, *et al.*, "Thin film lithium and lithium ion batteries", Solid State Ionics, Vol. 135, pp. 33 45, 2000.
- [18] D. A. Minkov, J. Phys. D: Appl. Phys. 22, 199 (1989).